Original Article

The identification of a PTEN-associated gene signature for the prediction of prognosis and planning of therapeutic strategy in endometrial cancer

Yuan Zhang[1,2], Li Li[3], Xiao-Ping Ke[3], Ping Liu[3]^

[1]Department of General Surgery, Yangpu Hospital, School of Medicine, Tongji University, Shanghai, China; [2]Department of Obstetrics, International Peace Maternity and Child Health Hospital, School of Medicine, Shanghai Jiao Tong University, Shanghai, China; [3]Department of Obstetrics and Gynaecology, Yangpu Hospital, School of Medicine, Tongji University, Shanghai, China

Contributions: (I) Conception and design: Y Zhang, P Liu; (II) Administrative support: P Liu; (III) Provision of study materials or patients: XP Ke; (IV) Collection and assembly of data: Y Zhang, L Li; (V) Data analysis and interpretation: Y Zhang, XP Ke; (VI) Manuscript writing: All authors; (VII) Final approval of manuscript: All authors.

Correspondence to: Ping Liu, MD, PhD. Department of Obstetrics and Gynaecology, Yangpu Hospital, School of Medicine, Tongji University, No. 450 Tengyue Road, Shanghai 200090, China. Email: Lpingyzx@163.com.

Background: Endometrial cancer (EC) is one of the most common malignancies among women. To improve the prognosis and treatment of EC, finding out a phosphatase and tensin homolog deleted on chromosome 10 (PTEN)-associated prognostic signature would be beneficial.

Methods: EC clinical data, genetic mutation data, and transcriptome data were downloaded from The Cancer Genome Atlas (TCGA) database. To clarify the specific PTEN-associated signature, cox regression analyses were performed. The clinical value of the selected signature on the overall survival (OS) and the secretoglobin family 2A member 1 (SCGB2A1)-independent analysis, immune and functional analysis were investigated respectively.

Results: Five hundred and fourteen EC samples were screened and PTEN mutation occupied 57%. Enrichment analysis indicated that mutant-type PTEN was enriched for pathways related to the upregulated human T-cell leukemia virus-1 (HTLV-1) infection and estrogen signaling pathway. SCGB2A1 was identified by cox regression analysis. Immune analysis exhibited significant immune infiltration with higher expression of T cells, B cells, and macrophage groups. Immune-checkpoint transcripts CD274 molecule (CD274), and cytotoxic T-lymphocyte associated protein 4 (CTLA4), hepatitis A virus cellular receptor 2 (HAVCR2), lymphocyte activation gene 3 (LAG3), programmed cell death 1 (PDCD1), PDCD1 ligand 2 (PDCD1LG2), T cell immunoreceptor with immunoglobulin and immunoreceptor tyrosine-based inhibition motif domains (TIGIT), and sialic acid binding immunoglobulin like lectin 15 (SIGLEC15) were discovered statistically different. In addition, the low-SCGB2A1 group had worse OS than the high-SCGB2A1 group. SCGB2A1 showed significant area under the curve (AUC) values in a time-dependent receiver operating characteristic (ROC) analysis. Prevalence of microsatellite instability (MSI) was detected and SCGB2A1 showed a negative correlation with EC. Immune checkpoint blockade (ICB) response indicated a worse immune response in the low-SCGB2A1 group. The distribution of one-class linear regression (OCLR) scores reflected the negative correlation between messenger RNA expression-based stemness index (mRNAsi) and prognostic gene expression. Furthermore, several SCGB2A1-related signaling pathways in EC were identified.

Conclusions: SCGB2A1 is a prognostic immunometabolic signature for patients with EC, which may help improve the prognosis and therapeutic effect.

^ ORCID: 0000-0001-7375-846X.

Keywords: Secretoglobin family 2A member 1 (SCGB2A1); phosphatase and tensin homolog deleted on chromosome 10 (PTEN); endometrial cancer (EC); prognosis; immunometabolic treatment

Submitted Aug 10, 2023. Accepted for publication Oct 29, 2023. Published online Dec 10, 2023.
doi: 10.21037/tcr-23-1436
View this article at: https://dx.doi.org/10.21037/tcr-23-1436

Introduction

It is indicated that the prognosis for different types of solid malignancies is relatively poor (1-3). As one of the most common malignancies among women, endometrial cancer (EC) is similarly rising in its incidence rate and its associated mortality (4). Minimally invasive surgery and adjuvant radiotherapy reduce loco-regional recurrence, and targeted chemotherapeutic strategies promote the prognosis of EC patients (5). In order to further improve the prognosis of patients more effectively, screening for a prognostic biomarker of the EC would be beneficial. Recent advances in bioinformatics analysis have provided efficient methods to investigate the prognostic biomarkers as diagnostic tools for clinical guidance and prevention of tumor progression (6-8).

As a dual phosphatase with both lipid and protein phosphatase activities, phosphatase and tensin homolog deleted on chromosome 10 (PTEN) is critical for cell metabolism and growth (9). One study has shown that tumor suppressor PTEN could inhibit the PI3K/AKT/mTOR signaling pathway (10). Besides, PTEN mutations play a role in immune regulation as an immune suppressor and accelerate cancer progression by mediating T cell dysfunction (11). In addition, biological function deficiency in the PTEN is always observed in various types of human cancers (12). In the past decades, there had been increasing interest in the close association between PTEN mutations and poor cancer survival rates, especially in EC (13-16). However, a systematic meta-analysis reported that PTEN showed low diagnostic usefulness in the differential diagnosis between benign and premalignant endometrial hyperplasia (17). Therefore, identifying a PTEN-associated signature would be helpful for improving the accuracy of prediction in prognosis and planning treatment strategy for EC.

The secretoglobin family 2A member 1 (SCGB2A1) is a small secreted uterine protein and the gene encoding this protein is located on chromosome 11q12.2 (18). It was reported that SCGB2A1 had been identified in epithelial cells of different organs and was closely related to cell secretion, tissue repair, inflammation and tumorigenesis (19). In the present study, SCGB2A1, as a prognostic signature in EC, was identified and the related immunometabolic mechanism was analyzed. The result of our study may be helpful to guide individualized therapies and improve the prognosis of EC patients in clinical practice. We present this article in accordance with the TRIPOD reporting checklist (available at https://tcr.amegroups.com/article/view/10.21037/tcr-23-1436/rc).

Highlight box

Key findings

- Secretoglobin family 2A member 1 (SCGB2A1) is a phosphatase and tensin homolog deleted on chromosome 10 (PTEN)-associated biomarker for the prediction of prognosis and planning of therapeutic strategy for patients with endometrial cancer (EC).

What is known and what is new?

- SCGB2A1 is known as a biomarker in several cancers.
- We found that the prognosis of patients with EC could be classified by PTEN-mutation status and high level of SCGB2A1 indicated a better prognosis. We found the characteristics of immune metabolism, as well as correlation between SCGB2A1 and related signaling pathways in EC.

What is the implication, and what should change now?

- SCGB2A1 could be applied as a potential target in the treatment for EC.
- We could create a novel targeted drug and bring innovation to the current treatment strategies.

Methods

Data collection

EC genetic mutation profile and clinical data were downloaded by searching the Project ID "TCGA-EC" from The Cancer Genome Atlas (TCGA) database (https://portal.gdc.cancer.gov/). There were 557 cases containing both clinical information and RNA sequence data selected and saved in the section of Cases and File Counts. We performed the R package "maftools" (v2.12.0, bioconductor.org/packages/release/bioc/html/maftools.html) to exhibit

the mutation data. Besides, MutsigCV represented mutation significance covariants.

Screening of differential expression genes (DEGs) and gene set enrichment analysis (GSEA)

The "limma" package (v3.52.4, bioconductor.org/packages/release/bioc/html/limma.html) of R software was performed to obtain DEGs between patients with and without PTEN mutations in EC. We utilized R package "clusterprofiler" (v3.0.4, https://rdocumentation.org/packages/clusterProfiler/versions/3.0.4) to investigate the Kyoto Encyclopedia of Genes and Genomes (KEGG) pathways and Gene Ontology (GO) functions. The threshold was set at "P<0.05".

Establishment of nomogram and prognosis of overall survival (OS) rate

The package "survtype" (v1.16.0, bioconductor.org/packages/release/bioc/html/survtype.html) of R software was utilized to perform the univariate and multivariate cox regression analyses. The P value and hazard ratio (HR), and 95% confidence interval (CI), were evaluated by the "forestplot" package (v1.10.1, https://rdocumentation.org/packages/forestplot/versions/1.10.1). The package "rms" (v6.1-0, https://rdocumentation.org/packages/rms/versions/6.1-0) of R software was performed to exhibit the risk factors and assessed the 1-, 3-, and 5-year OS rate in the nomogram. If Kaplan-Meier curves crossed over, a two-stage procedure was performed using the R package "TSHRC" (v0.1-6, https://cran.r-project.org/web/packages/TSHRC/index.html). The R package "ggrisk" (v1.3, https://cran.r-project.org/web/packages/ggrisk/index.html) was performed to analyze the risk score, survival status and heatmap. The expression type of SCGB2A1 in different groups was calculated by the Chi-squared test. We utilized R package "ggplot2" (v3.3.3, https://rdocumentation.org/packages/ggplot2/versions/3.3.3) to complete all the above analytical methods. The threshold was set at "P<0.05".

Prediction of microsatellite instability (MSI) score and immune checkpoint blockade (ICB) response, Sankey diagram, and one-class linear regression (OCLR) scores

We conducted the Spearman's correlation analysis to reveal the correlation between quantitative variables without a normal distribution. Potential ICB response was predicted by the Tumor Immune Dysfunction and Exclusion (TIDE) algorithm (20) and package "ggplot2" (v3.3.3, https://rdocumentation.org/packages/ggplot2/versions/3.3.3) and "ggpubr" (v0.4.0, https://rdocumentation.org/packages/ggpubr/versions/0.4.0). Sankey diagram was established with the R software package "ggalluvial" (v0.12.5, https://rdocumentation.org/packages/ggalluvial/versions/0.12.5). We calculated messenger RNA expression-based stemness index (mRNAsi) which was constructed by Malta *et al.* (21) by Spearman's correlation analysis and OCLR algorithm.

Specimens collection

We obtained the surgically resected tumor tissues in December 2020 from Yangpu Hospital (Shanghai, China). The inclusion criteria included: (I) pathological diagnosis (including all histotypes of EC); (II) no prior treatment received; (III) surgical resection accepted without distant disease. The exclusion criteria included: surgical resection rejected. Our study was approved by the Ethics Committee of Yangpu Hospital (No. YZX20201105A1) and was conducted in accordance with the Declaration of Helsinki (as revised in 2013). All patients provided written informed consent.

Immunohistochemistry

The procedure was conducted as previously described (22). All EC tissues and adjacent normal tissues were fixed in 4% phosphate-buffered formalin for at least 24 hours. And then tissues were paraffin-embedded. The 4-μm-thick sections were dewaxed with xylene and rehydrated with descending graded alcohol. Heat-mediated antigen retrieval was performed at 98 ℃ for 20 min. After blocking non-specific sites with 5% goat serum at 37 ℃ for 30 min, the primary antibody (1:200; #TP51210, Abmart, China) was incubated with the sections overnight at 4 ℃ and secondary antibodies (1:2,000, #Ab205718, Abcam, UK) for 1 h at room temperature. Antibodies were visualized using 3,3'-diaminobenzidine and counterstained using Meyer's hematoxylin for 2 min at room temperature. An increasing gradient of alcohols was used to dehydrate. Immunostaining results were observed using a microscope (Olympus BX51, Japan).

Western blotting assay

The EC tissues and adjacent normal tissues were ground

using rapidly rotating magnetic bead in lysis solution (RIPA, Radio-Immunoprecipitation Assay buffer; Thermo Fisher Scientific, USA) and 1% (v/v) protease inhibitors (cat. no. P8340; Merck, USA). Protein Quantification kit (BCA Assay; Beyotime, China) was applied to standardized the protein concentration. After blocked in Tris-Buffer Saline Tween 20 at room temperature for 60 min, membranes were incubated with anti-SCGB2A1 primary antibody (1:1,000; #PU615103, Abmart) overnight at 4 ℃. The level of actin (1:5,000; #T0022, Abmart) protein expression was measured as an internal standard. The next day, membranes were incubated with secondary antibody for 1 h at room temperature: anti-Rabbit (1:2,000; #ab6721, Abcam), anti-Mouse (1:2,000; #ab205719, Abcam). Enhanced chemiluminescence reagent (SuperSignal™ West Atto Ultimate Sensitivity Substrate; Thermo Fisher Scientific) was used for chemiluminescence detection. The density of protein band was measured using Image J software (NIH, Bethesda, MD, USA).

Immune metabolism prediction

We integrated the package "immunedeconv" (v2.0.3, https://rdocumentation.org/packages/immunedeconv/versions/2.0.3) with the EPIC algorithm to evaluate the immune infiltration and immune cell score. CD274 molecule (CD274), cytotoxic T-lymphocyte associated protein 4 (CTLA4), hepatitis A virus cellular receptor 2 (HAVCR2), lymphocyte activation gene 3 (LAG3), programmed cell death 1 (PDCD1), PDCD1 ligand 2 (PDCD2LG2), T cell immunoreceptor with immunoglobulin and immunoreceptor tyrosine-based inhibition motif domains (TIGIT), and sialic acid binding immunoglobulin like lectin 15 (SIGLEC15) were screened to be target transcripts. R package "ggplot2" (v0.4.0, https://rdocumentation.org/packages/ggpubr/versions/0.4.0) and "pheatmap" (v1.0.12, https://rdocumentation.org/packages/pheatmap/versions/1.0.12) were performed to analyze the above immune analysis.

Evaluation of correlation between the target gene and pathway scores

We utilized the gene set variation analysis (GSVA) package (v1.20.0, https://rdocumentation.org/packages/GSVA/versions/1.20.0) and analyzed the correlation between the target gene and pathway scores by Spearman correlation.

Statistical analysis

We utilized R software (version 4.0.3) in all statistical analysis. Besides, we investigated the significance of differences between subgroups by two-tailed Student's *t*-test. The correlation between risk score and clinicopathological parameters was analyzed by the one-way analysis of variance (ANOVA) test or Student's *t*-test. The Wilcoxon test was performed to compare the data of two groups and the Kruskal-Wallis test was utilized to compare the data of more than three groups. "P<0.05" was considered statistically significant.

Results

PTEN mutation was predominant in EC

Figure 1 presents the workflow of our study. A total of 514 samples with a gene mutation were selected from the TCGA database. The identified genes, such as PTEN (57%), phosphatidylinositol-4,5-bisphosphate 3-kinase catalytic subunit alpha (PIK3CA; 48%), titin (TTN; 44%), AT-rich interaction domain 1A (ARID1A; 43%), tumor protein p53 (TP53; 36%), mucoprotein 16 (MUC16; 30%), phosphoinositide-3-kinase regulatory subunit 1 (PIK3R1; 30%), lysine methyltransferase 2D (KMT2D; 27%), CCCTC-binding factor (CTCF; 25%), CUB and Sushi multiple domains 3 (CSMD3; 24%), showed a higher level of mutation frequency than other genes and they were visualized using a horizontal histogram (*Figure 2A*). In addition, missense mutation was the most frequent mutation type, and single nucleotide polymorphism occupied a large proportion compared with deletion or insertion (*Figure 2B,2C*). The most distinct part of single nucleotide variants class was C>T (*Figure 2D*). *Figure 2E* shows the number of mutations in each specimen. Different types of mutations were represented by different colors in the box diagram (*Figure 2F*). The top 10 mutant genes in *Figure 2G* are shown by the stacked barplot. *Figure 2H* shows the highly mutated genes in EC using a lollipop plot.

DEGs in EC were classified according to PTEN status

DEGs were divided into the PTEN mutant and wild type groups. A total of 111 upregulated and 128 downregulated

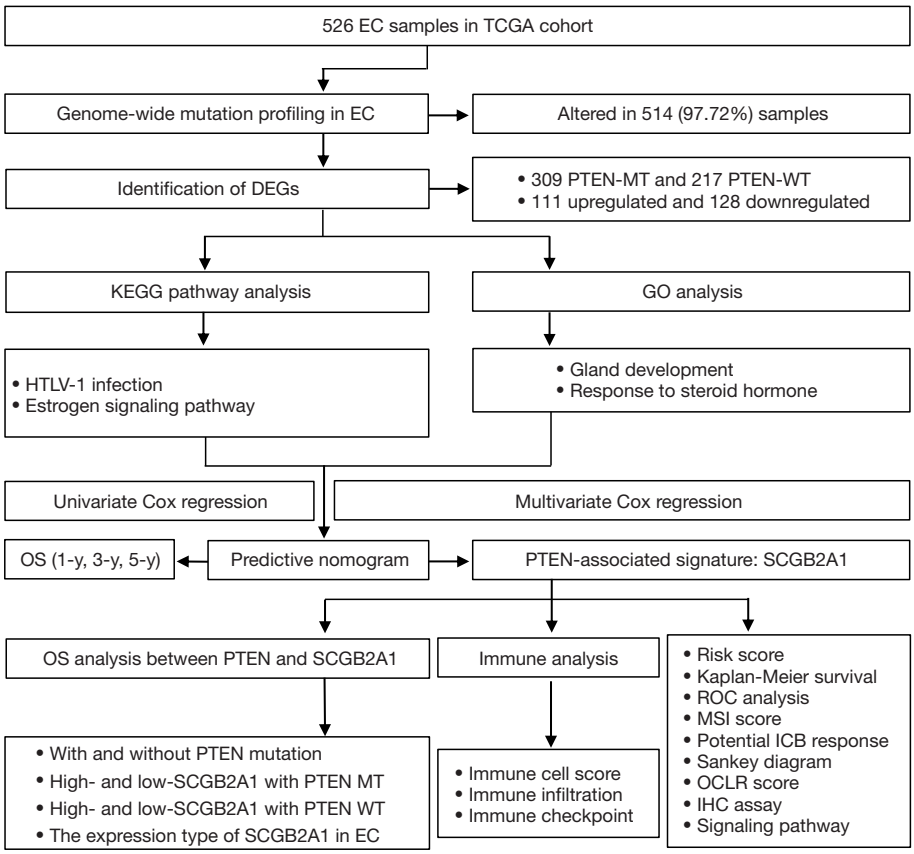

Figure 1 Workflow of the study. EC, endometrial cancer; TCGA, the cancer genome atlas; DEGs, differential expression genes; PTEN, phosphatase and tensin homolog deleted on chromosome 10; MT, mutant type; WT, wild type; KEGG, Kyoto Encyclopedia of Genes and Genomes; GO, Gene Ontology; HTLV-1, human T-cell leukemia virus 1; OS, overall survival; SCGB2A1, secretoglobin family 2A member 1; ROC, receiver operating characteristic; MSI, microsatellite instability; ICB, immune checkpoint blockade; OCLR, one-class linear regression; IHC, immunohistochemistry.

genes were investigated (*Figure 3A-3F*). DEGs were mostly enriched in pathways related to the upregulated human T-cell leukemia virus-1 (HTLV-1) infection and estrogen signaling pathway (*Figure 3C,3D*). In addition, gland development and response to steroid hormone were the most enriched terms of the PTEN mutation (*Figure 3E,3F*).

Establishment of a predictive nomogram

Nineteen upregulated genes and nineteen downregulated genes, age, race, pTNM_stage and grade were exhibited by cox regression analysis using "forestplot" package (*Figure 4A,4B*). The signatures in the predictive nomogram (*Figure 4C*, left), including SCGB2A1 and cyclin dependent kinase inhibitor 2A, satisfied the standard of risk assessment. Besides, the 1-, 3- and 5- year OS rates were predicted precisely (*Figure 4C*, right).

PTEN and SCGB2A1 status was closely associated with the prognosis of EC

The poor prognosis of patients with EC was closely associated with PTEN mutations compared with those in PTEN wild-type group (P<0.05; *Figure 5A*). To explore whether SCGB2A1 was independent of the PTEN mutation status, patients were separated into high- and low-SCGB2A1 groups based on PTEN mutation status. The research revealed that patients with low-SCGB2A1 were significantly correlated with a worse survival in both the mutant and wild-type PTEN groups compared with the high-SCGB2A1 group (P<0.05; *Figure 5B,5C*). The cross curves in *Figure 5C* had been determined to be significantly different (P<0.05) by performing a two-stage procedure, using the P 'TSHRC' package of the R software.

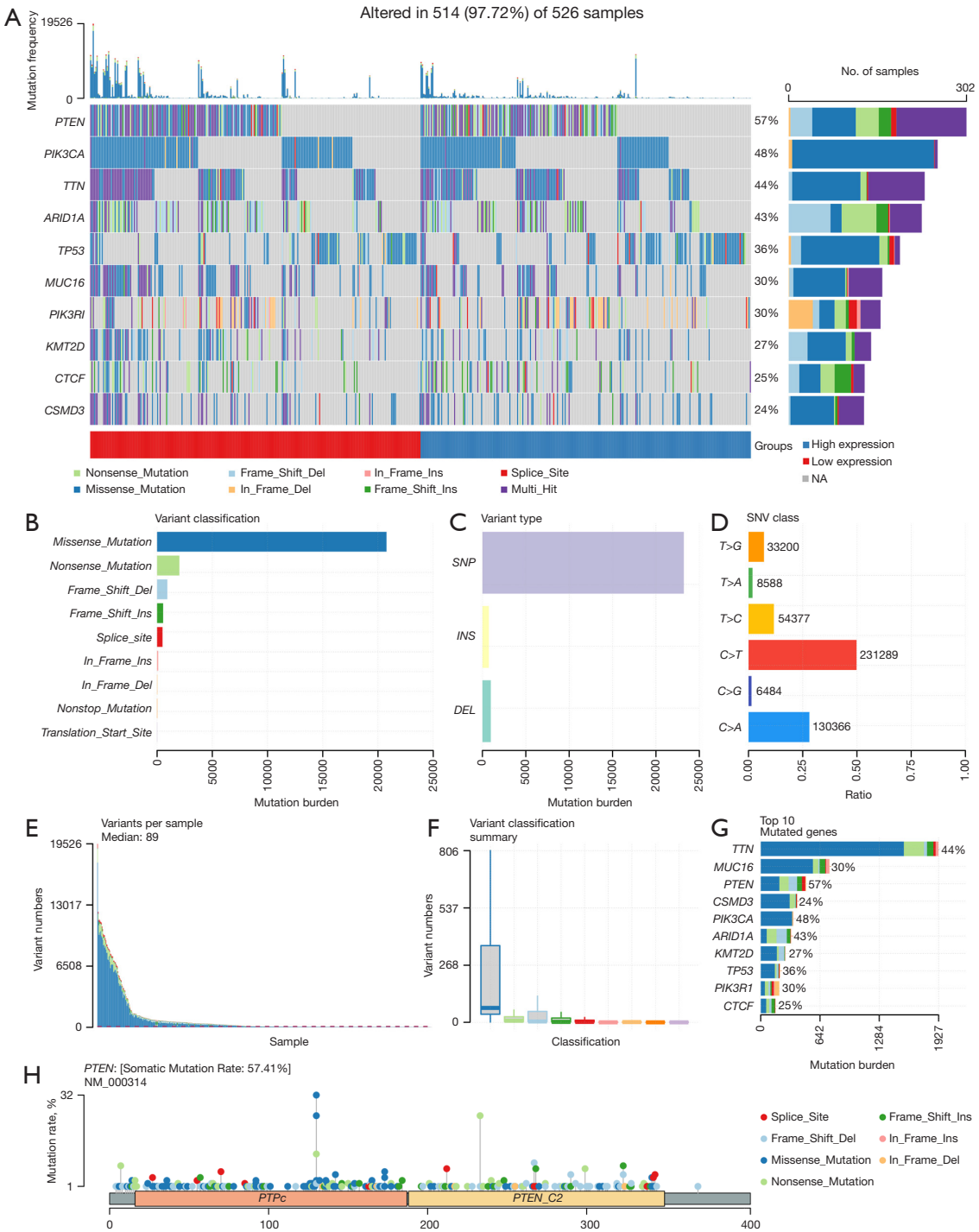

Figure 2 Gene mutations in EC. (A) Oncoplot exhibited the somatic landscape of the EC specimens. Genes are ordered by their mutation frequency and samples are ordered according to disease histology as indicated by the annotation bar (bottom). The bar plot (right) shows log10 transformed Q-values estimated by MutSigCV. (B-G) A cohort summary plot showed the distribution of variants classified by (B) variant classification, (C) type, and (D) SNV class: A, adenine; T, thymine; C, cytosine; G, guanine. The bottom part indicated the mutation load of each (E) specimen and (F) variant classification type. The top 10 mutant genes were exhibited by (G) a stacked barplot. (H) Mutation distribution and protein domains for PTEN in EC were exhibited by Lollipop plot. EC, endometrial cancer; PTEN, phosphatase and tensin homolog deleted on chromosome 10; PIK3CA, phosphatidylinositol-4,5-bisphosphate 3-kinase catalytic subunit alpha; TTN, titin; ARID1A, AT-rich interaction domain 1A; TP53, tumor protein p53; MUC16, mucoprotein 16; PIK3R1, phosphoinositide-3-kinase regulatory subunit 1; KMT2D, lysine methyltransferase 2D; CTCF, CCCTC-binding factor; CSMD3, CUB and sushi multiple domains 3; NA, not applicable; SNP, single nucleotide polymorphism; INS, insertion mutation; DEL, deletion mutation; SNV, stable nuclear variant.

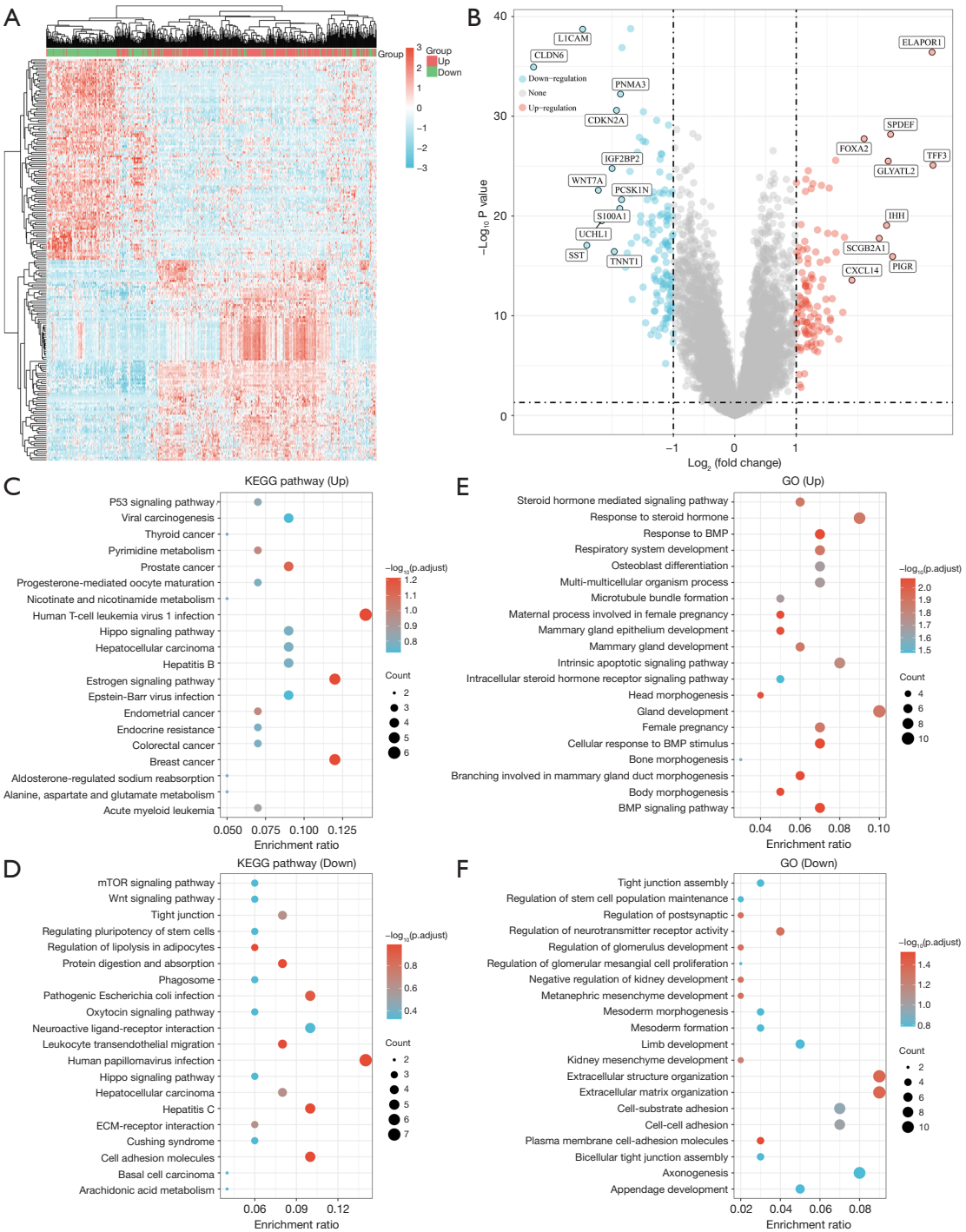

Figure 3 DEGs with and without PTEN mutations in EC. (A) Heatmap of DEGs. (B) Volcano plots of DEGs. (C-F) The enriched KEGG pathways (C, upregulated; D, down-regulated) and GO analysis (E, upregulated; F, downregulated). P<0.05 was considered to be enriched to a significantly different pathway. DEGs, differential expression genes; EC, endometrial cancer; PTEN, phosphatase and tensin homolog deleted on chromosome 10; KEGG, Kyoto Encyclopedia of Genes and Genomes; GO, Gene Ontology; BMP, bone morphogenetic protein; L1CAM, L1 cell adhesion molecule; CLDN6, claudin 6; PNMA3, PNMA family member 3; CDKN2A, cyclin dependent kinase inhibitor 2A; IGF2BP2, insulin like growth factor 2 MRNA binding protein 2; WNT7A, Wnt family member 7A; PCSK1N, proprotein convertase subtilisin/kexin type 1 inhibitor; S100A1, S100 calcium binding protein A1; UCHL1, ubiquitin c-terminal hydrolase L1; SST, somatostatin; TNNT1, troponin T1, slow skeletal type; ELAPOR1, endosome-lysosome associated apoptosis and autophagy regulator 1; SPDEF, SAM pointed domain containing ETS transcription factor; FOXA2, forkhead box A2; TFF3, trefoil factor 3; GLYATL2, glycine-N-acyltransferase like 2; IHH, Indian hedgehog signaling molecule; CXCL14, C-X-C motif chemokine ligand 14; PIGR, polymeric immunoglobulin receptor; ECM, extracellular matrix.

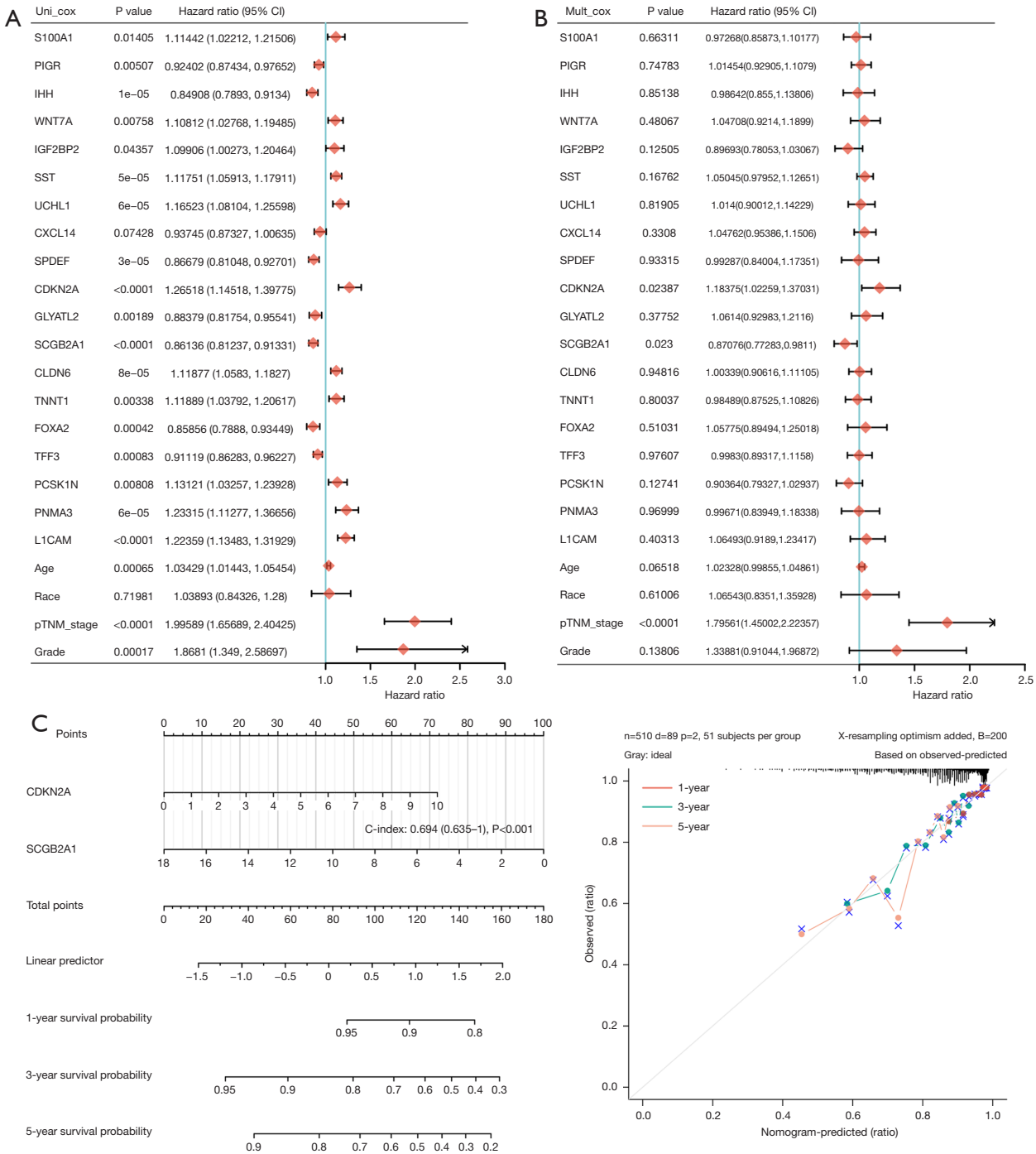

Figure 4 DEGs-based prognostic signature. (A,B) Prognostic values of DEGs by univariate and multivariate cox regression analysis. (C) Nomogram to predict the 1-, 3- and 5-year OS rate of patients. The grey line represents the ideal nomogram. CI, confidence interval; DEGs, differential expression genes; OS, overall survival.

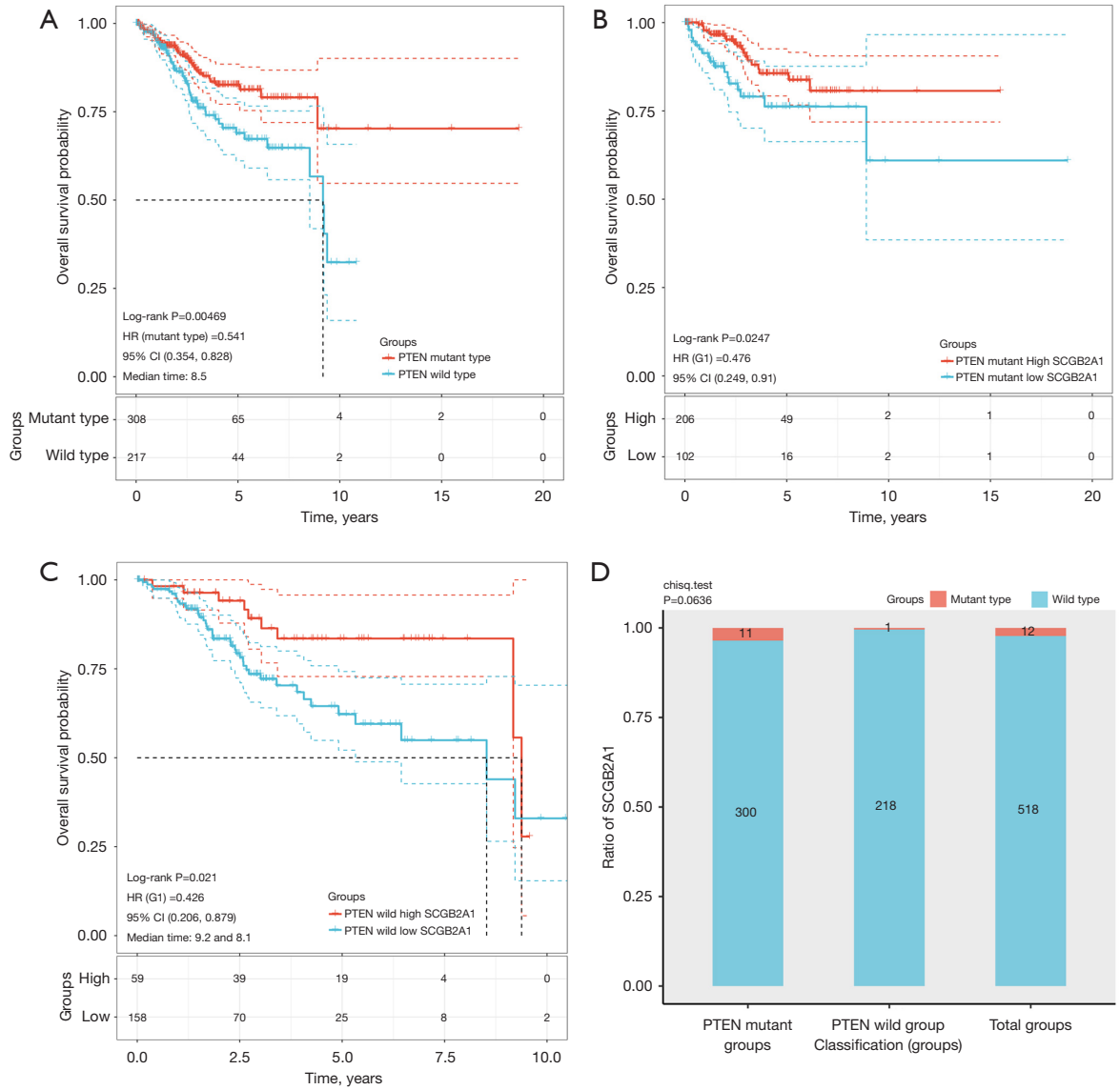

Figure 5 K-M analysis of OS time. (A) K-M survival according to PTEN status. (B) K-M survival in the PTEN mutation group by SCGB2A1 status. (C) K-M survival in the PTEN wild group by SCGB2A1 status. (D) The different types of SCGB2A1 expression in different groups of EC (χ^2 test). Dotted lines represent the confidence interval. PTEN, phosphatase and tensin homolog deleted on chromosome 10; HR, hazard ratio; CI, confidence interval; OS, overall survival; K-M, Kaplan-Meier; SCGB2A1, secretoglobin family 2A member 1; EC, endometrial cancer.

Furthermore, it was discovered that wild-type SCGB2A1 is highly prevalent in EC patients by Chi-squared (χ^2) test (*Figure 5D*). Dotted lines in *Figure 5A-5C* represent the CI.

Predictive value of the SCGB2A1 gene

To separate the patients into the high-SCGB2A1 (n=271) and low-SCGB2A1 (n=271) groups, the risk score and the median cut-off point (*Figure 6A*, up) were calculated. The survival status of all patients with EC is shown in *Figure 6A*, middle. The heatmap illustrated the gene expression profile of SCGB2A1 (*Figure 6A*, down). Compared with the high-SCGB2A1 group, a worse OS time was observed in the low-SCGB2A1 group, as shown by Kaplan-Meier survival curves (*Figure 6B*). In addition, a time-dependent receiver operating characteristic (ROC) analysis was performed

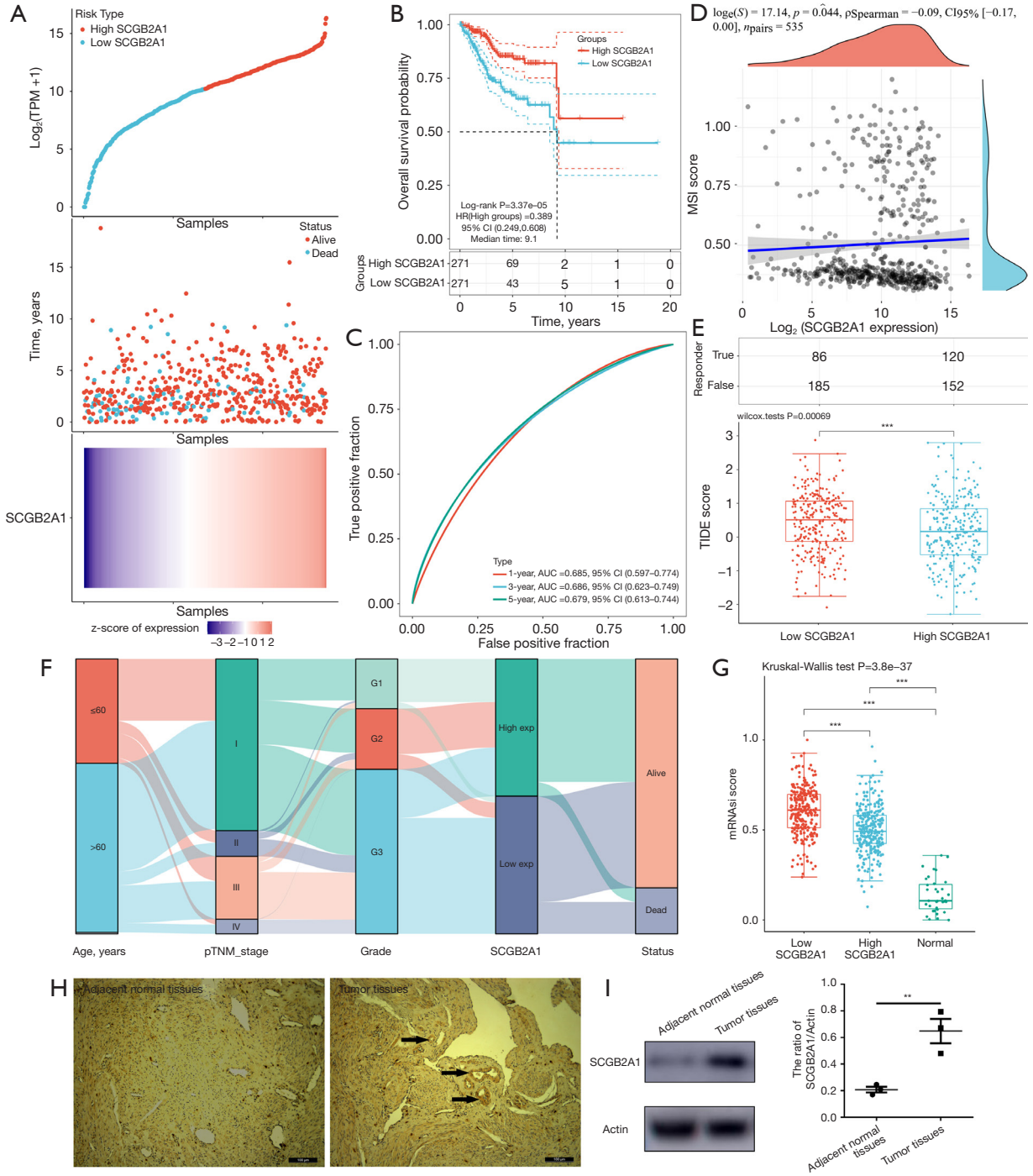

Figure 6 The value of the predictive signature SCGB2A1 for EC. (A) Curve of risk score (up); survival status of the patients (middle); heatmap of the SCGB2A1 expression profile (down). (B) K-M survival analysis of patients with EC by SCGB2A1 status. Dotted lines represent the confidence interval. (C) Time-dependent ROC analysis. (D) MSI score. (E) Potential ICB responses. (F) Sankey diagram. (G) OCLR scores. (H) Representative images of immunohistochemistry staining exhibited the expression level of SCGB2A1 in clinical EC tissues. The left image represented the adjacent normal tissue and the right image represented the tumor tissue. The expression of SCGB2A1 was strongly positive in the brown area, which was indicated by the black arrows. (I) Western blot was used to detect the expression of SCGB2A1 between adjacent normal tissues and tumor tissues. Column showing that SCGB2A1 was detected higher in tumor tissues. The data represent means ± SEM. Scare bar, 100 μm. **, P<0.01; ***, P<0.001. SCGB2A1, secretoglobin family 2A member 1; EC, endometrial cancer; K-M, Kaplan-Meier; ROC, receiver operating characteristic; MSI, microsatellite instability; ICB, immune checkpoint blockade; OCLR, one-class linear regression; SEM, standard error of the mean.

to identify the significant area under the ROC curve (*Figure 6C*), which exhibited the ability of SCGB2A1 in predicting the 1-, 3- and 5-year OS. MSI prevalence was found negatively correlated with the gene expression of SCGB2A1 (*Figure 6D*). The immune scores in the low-SCGB2A1 group showed a lower-level ICB response, as compared with the high-SCGB2A1 group (*Figure 6E*). The distribution of SCGB2A1 expression in different characteristic variables and different types or stages was shown in a Sankey diagram (*Figure 6F*). The distribution of OCLR scores revealed that low SCGB2A1 was strongly positively correlated with a high mRNAsi score (*Figure 6G*). Furthermore, the level of SCGB2A1 expression was higher in tumor tissues than adjacent normal tissues by immunohistochemistry (*Figure 6H*) and western blotting assay (*Figure 6I*).

Differential immune analysis

Thirty-eight types of immune cells were finally included in the comparison and we explored the distribution of different immune scores (*Figure 7A*) and the percentage abundance of immune infiltration (*Figure 7B*). As shown in *Figure 7*, 31 types of immune cells were found statistically different from other rest 7 types. In addition, a higher level of T cell, B cell and macrophage groups was discovered, which indicated a distinctive immune microenvironment. In terms of the expression of immune checkpoints, CD274, CTLA4, HAVCR2, LAG3, PDCD1, PDCD1LG2, TIGIT and SIGLEC15 were found to be significantly different (*Figure 7C*).

The correlation between SCGB2A1 and pathway scores

The correlations were classified according to pathway score by GSVA analysis across all EC samples. The proportions of pathway score greatly varied among different EC samples (*Figure 8A-8R*). Some pathways had a high score: genes upregulated by reactive oxygen species (ROS), cellular response to hypoxia, extracellular matrix (ECM) related genes, collagen formation and inflammatory response, angiogenesis, tumor proliferation and apoptosis, DNA repair and replication, P53 pathway, MYC proto-oncogene, bHLH transcription factor (MYC targets) and G2M checkpoint.

Discussion

Current study indicated that the tumor microenvironment was affected by the interactive crosstalk between tumor cells and stromal cells (23). Aquila *et al.* (24) had proposed that PTEN played an important role in metabolic reprogramming and tumor/stroma interactions. In our research, we found that PTEN had a high mutation frequency in patients with EC (*Figure 2*). We further discovered that SCGB2A1 was an effective independent prognostic biomarker for EC and could be affected by PTEN mutation status (*Figures 4,5*). In a study conducted by Kim *et al.* (25), SCGB2A1 was identified as a PIK3CA-interacting protein in breast-invasive carcinoma, which inhibited PI3K-AKT signaling pathway. In addition, Yan *et al.* (26) proposed that SCGB2A1 was a critical tumor suppressor and a potential prognostic marker in gastric cancer. In our research, the specific function of SCGB2A1 in prognostic value and immunometabolic mechanism in EC were revealed, which could provide a potential therapeutic target in EC.

One study was completed by Bellone *et al.* (27), in which it was reported that SCGB2A1 was a top differentially expressed gene in all major histological types of ovarian cancers. In our study, we detected the higher expression of SCGB2A1 in tumor tissues than normal tissues in EC (*Figure 6H,6I*). Zhang *et al.* (18) reported that SCGB2A1 overexpression in breast cancer cells inhibited cell activity and promoted cell apoptosis. According to our results, we found that patients with low-SCGB2A1 were significantly correlated with a worse EC survival, which revealed that SCGB2A1 was a protective factor in EC (*Figure 6*). However, Munakata *et al.* (28) proposed that SCGB2A1 promoted colorectal cancer cell proliferation and decreased chemosensitivity to chemotherapy drugs. These results indicated that SCGB2A1 might function as tumor suppressor in the breast cancer and gynaecological tumors. Therefore, we hypothesized that SCGB2A1 could be involved in estrogen metabolism and acts as a potential biomarker for patients with EC.

Immunotherapy could activate the immune cells to attack and clear tumor cells (29). The identification of immune subtypes in EC tissues could be beneficial to clarify the unique immune microenvironment and predict the prognosis of EC patients (30). In our study, distinct immune infiltration with a higher level of T cells, B cells and macrophage groups were identified (*Figure 7A,7B*). These immune cells could be explored to generate effective chimeric antigen receptor (CAR) immunotherapy. However, CAR T cells immunotherapy in solid tumors lags behind significantly. Therefore, it is meaningful to develop CAR

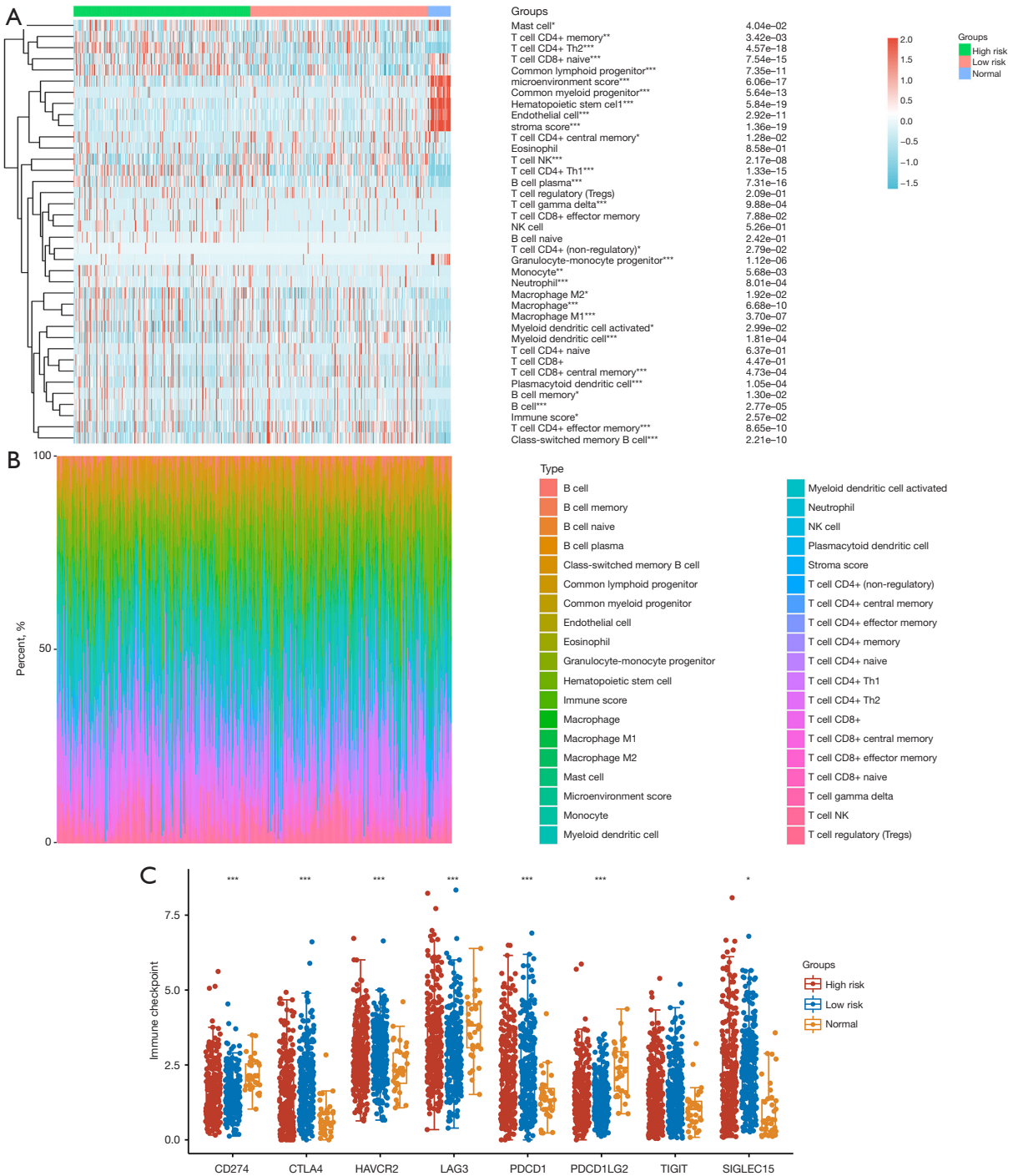

Figure 7 Analysis of immune metabolism. (A) Heat map of immune cell score. (B) Percentage abundance of tumor-infiltrating immune cells. The abscissa represents the sample and the ordinate represents the percentage of immune cell content in a single sample. (C) The expression distribution of immune checkpoints. Statistically significant differences among three groups were tested using Kruskal-Wallis test. *, P<0.05; **, P<0.01; ***, P<0.001. CD274, CD274 molecule; CTLA4, cytotoxic T-lymphocyte associated protein 4; HAVCR2, hepatitis A virus cellular receptor 2; LAG3, lymphocyte activating gene 3; PDCD1, programmed cell death 1; PDCD1LG2, PDCD1 ligand 2; TIGIT, T cell immunoreceptor with immunoglobulin and immunoreceptor tyrosine-based inhibition motif domains; SIGLEC15, sialic acid binding immunoglobulin like lectin 15.

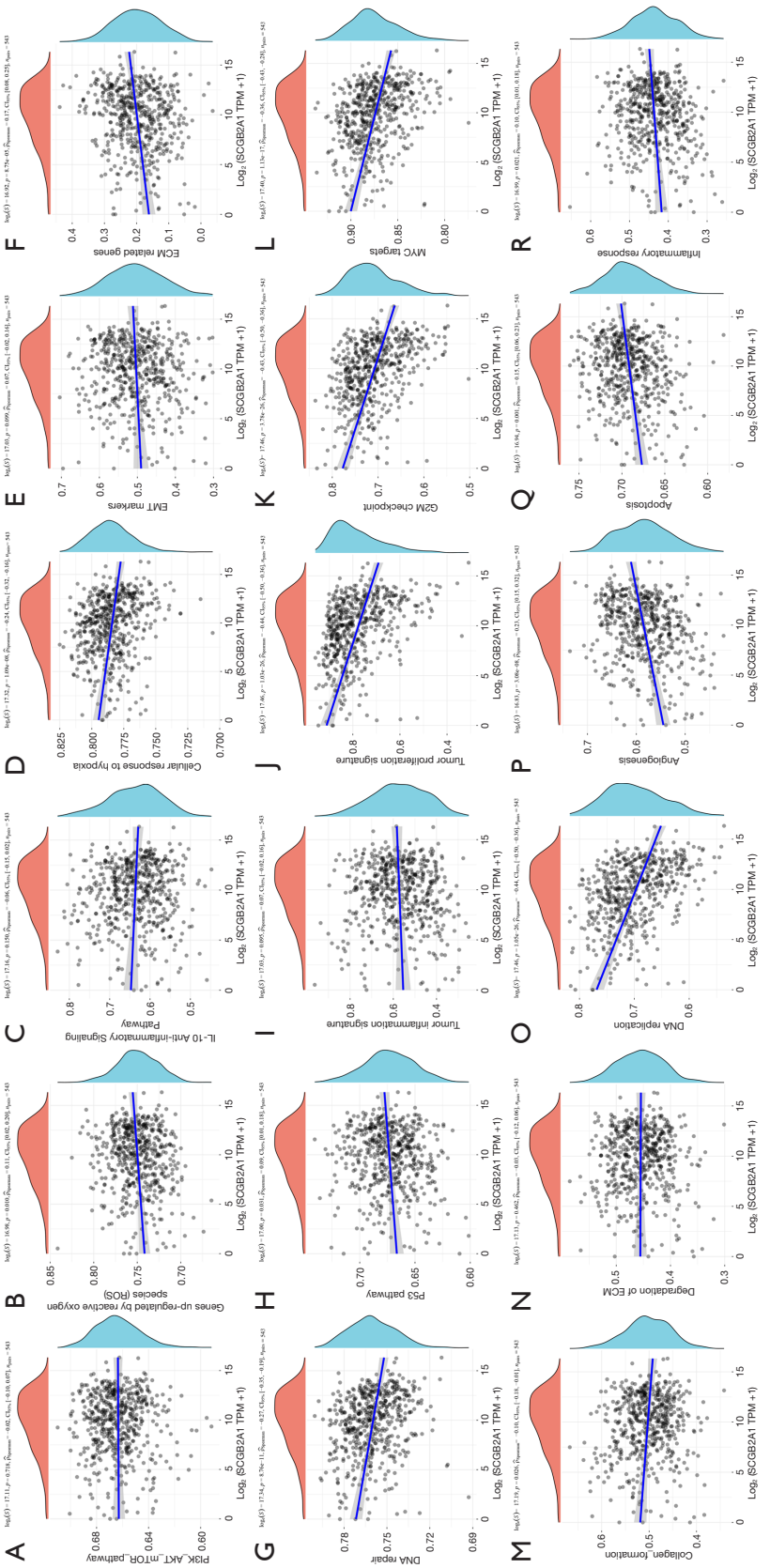

Figure 8 Correlation between SCGB2A1 and pathway score in EC. (A) PI3K/AKT/mTOR pathway. (B) Genes upregulated by ROS. (C) IL-10 anti-inflammatory signaling pathway. (D) Cellular response to hypoxia. (E) EMT markers. (F) ECM-related genes. (G) DNA repair. (H) P53 pathway. (I) Tumor inflammation signature. (J) Tumor proliferation signature. (K) G2M checkpoint. (L) MYC targets. (M) Collagen formation. (N) Degradation of ECM. (O) DNA replication. (P) Angiogenesis. (Q) Apoptosis. (R) Inflammatory response. The abscissa represents the expression of SCGB2A1 and the ordinate represents the pathway score. The density curve on the right represents the trend of pathway immune score and the upper represents the trend of the gene expression. IL-10, interleukin 10; SCGB2A1, secretoglobin family 2A member 1; EC, endometrial cancer; ROS, reactive oxygen species; EMT, epithelial mesenchymal transition; ECM, extracellular matrix.

macrophages for cancer immunotherapy (31). In fact, 30% of primary EC were MSI high (MSI-H)/hypermutated and 13% to 30% of recurrent EC were MSI-H or mismatch repair deficient. Thus, ICB has been explored as an effective therapy (32). Furthermore, the effect of immunotherapy would be enhanced in combination with multiple immunocheckpoint inhibitors (29). In the present study, six immune checkpoints, including CD274, CTLA4, HAVCR2, LAG3, PDCD1 and PDCD1LG2 were found to be statistically different (*Figure 7C*). Besides, potential functional pathways were explored using GSVA analysis (*Figure 8*) and it was found that SCGB2A1 could impair mitochondrial metabolism, which led to the increase of ROC and abnormal cellular response to hypoxia. In addition, the invasion and metastasis of tumors could be affected by a higher SCGB2A1 expression, which induced ECM change and collagen formation. In our study, inflammatory response, angiogenesis, tumor proliferation and apoptosis, DNA repair and replication, P53 pathway, MYC targets and G2M checkpoints were all affected by a higher SCGB2A1 expression, which might be helpful to the further research. The negative correlation between SCGB2A1 expression and MSI, ICB response, and mRNAsi further highlighted a convincing evidence to guide clinical treatment. Although the standard treatment for EC now is still surgery or chemo- and radiotherapy, hormone therapy and immunotherapy would be the most promising therapeutic approach for EC patients (33).

In our study, we analyzed all histotypes of EC without detailed histological classification, because the value of histological type was less certain and EC patients with similar histology might have different outcomes (34). However, lymph vascular space invasion (LVSI) might be regarded as the valuable supplement, which was defined as the presence of tumour cells within an endothelial-lined space that lies outside the invasive border. Researchers had reported that LVSI increased the risk of death due to EC and recurrent or progressive disease by 1.5–2 times (35). Besides, sentinel node mapping played a critical role in identifying nodal involvement in EC patients of different risk levels (36). At the same time, molecular and genomic profiling showed the possibility to improve the risk stratification and management of EC (37). In addition, metabolic syndrome was closely associated with poor prognosis in EC patients (38). Furthermore, Glasgow prognostic score and C-reactive protein-to-albumin ratio also had great prognostic value in EC patients (39).

Conclusions

Above all, SCGB2A1 was identified as an effective immune-metabolism biomarker for EC patients. Due to the limited amounts of clinical data, further independent clinical trials and experimental research are needed to confirm the predictive performance and clarify the specific molecular mechanism.

Acknowledgments

Funding: None.

Footnote

Reporting Checklist: The authors have completed the TRIPOD reporting checklist. Available at https://tcr.amegroups.com/article/view/10.21037/tcr-23-1436/rc

Data Sharing Statement: Available at https://tcr.amegroups.com/article/view/10.21037/tcr-23-1436/dss

Peer Review File: Available at https://tcr.amegroups.com/article/view/10.21037/tcr-23-1436/prf

Conflicts of Interest: All authors have completed the ICMJE uniform disclosure form (available at https://tcr.amegroups.com/article/view/10.21037/tcr-23-1436/coif). The authors have no conflicts of interest to declare.

Ethical Statement: The authors are accountable for all aspects of the work in ensuring that questions related to the accuracy or integrity of any part of the work are appropriately investigated and resolved. The study was approved by the Ethics Committee of Yangpu Hospital (No. YZX20201105A1) and was conducted in accordance with the Declaration of Helsinki (as revised in 2013). All patients provided written informed consent.

References

1. Reig M, Forner A, Rimola J, et al. BCLC strategy for prognosis prediction and treatment recommendation: The 2022 update. J Hepatol 2022;76:681-93.
2. Wadowska K, Bil-Lula I, Trembecki Ł, et al. Genetic Markers in Lung Cancer Diagnosis: A Review. Int J Mol Sci 2020;21:4569.
3. Baidoun F, Elshiwy K, Elkeraie Y, et al. Colorectal Cancer Epidemiology: Recent Trends and Impact on Outcomes. Curr Drug Targets 2021;22:998-1009.
4. Lu KH, Broaddus RR. Endometrial Cancer. N Engl J Med 2020;383:2053-64.
5. Crosbie EJ, Kitson SJ, McAlpine JN, et al. Endometrial cancer. Lancet 2022;399:1412-28.
6. Gong L, Zhang D, Dong Y, et al. Integrated Bioinformatics Analysis for Identificating the Therapeutic Targets of Aspirin in Small Cell Lung Cancer. J Biomed Inform 2018;88:20-8.
7. Chen L, Wang C, Sun H, et al. The bioinformatics toolbox for circRNA discovery and analysis. Brief Bioinform 2021;22:1706-28.
8. Wang Y, Yang C, Li W, et al. Identification of colon tumor marker NKD1 via integrated bioinformatics analysis and experimental validation. Cancer Med 2021;10:7383-94.
9. Chen CY, Chen J, He L, et al. PTEN: Tumor Suppressor and Metabolic Regulator. Front Endocrinol (Lausanne) 2018;9:338.
10. Parsons R. Discovery of the PTEN Tumor Suppressor and Its Connection to the PI3K and AKT Oncogenes. Cold Spring Harb Perspect Med 2020;10:a036129.
11. Sun Y, Lu D, Yin Y, et al. PTENα functions as an immune suppressor and promotes immune resistance in PTEN-mutant cancer. Nat Commun 2021;12:5147.
12. Álvarez-Garcia V, Tawil Y, Wise HM, et al. Mechanisms of PTEN loss in cancer: It's all about diversity. Semin Cancer Biol 2019;59:66-79.
13. Chida K, Kawazoe A, Kawazu M, et al. A Low Tumor Mutational Burden and PTEN Mutations Are Predictors of a Negative Response to PD-1 Blockade in MSI-H/dMMR Gastrointestinal Tumors. Clin Cancer Res 2021;27:3714-24.
14. Wise HM, Hermida MA, Leslie NR. Prostate cancer, PI3K, PTEN and prognosis. Clin Sci (Lond) 2017;131:197-210.
15. Ngeow J, Sesock K, Eng C. Breast cancer risk and clinical implications for germline PTEN mutation carriers. Breast Cancer Res Treat 2017;165:1-8.
16. Raffone A, Travaglino A, Saccone G, et al. PTEN expression in endometrial hyperplasia and risk of cancer: a systematic review and meta-analysis. Arch Gynecol Obstet 2019;299:1511-24.
17. Raffone A, Travaglino A, Saccone G, et al. Loss of PTEN expression as diagnostic marker of endometrial precancer: A systematic review and meta-analysis. Acta Obstet Gynecol Scand 2019;98:275-86.
18. Zhang L, Yan X, Yu S, et al. LINC00365-SCGB2A1 axis inhibits the viability of breast cancer through targeting NF-κB signaling. Oncol Lett 2020;19:753-62.
19. Lu X, Wang N, Long XB, et al. The cytokine-driven regulation of secretoglobins in normal human upper airway and their expression, particularly that of uteroglobin-related protein 1, in chronic rhinosinusitis. Respir Res 2011;12:28.
20. Jiang P, Gu S, Pan D, et al. Signatures of T cell dysfunction and exclusion predict cancer immunotherapy response. Nat Med 2018;24:1550-8.
21. Malta TM, Sokolov A, Gentles AJ, et al. Machine Learning Identifies Stemness Features Associated with Oncogenic Dedifferentiation. Cell 2018;173:338-354.e15.
22. Xu F, Lin H, He P, et al. A TP53-associated gene signature for prediction of prognosis and therapeutic responses in lung squamous cell carcinoma. Oncoimmunology 2020;9:1731943.
23. Sahoo SS, Zhang XD, Hondermarck H, et al. The Emerging Role of the Microenvironment in Endometrial Cancer. Cancers (Basel) 2018;10:408.
24. Aquila S, Santoro M, Caputo A, et al. The Tumor Suppressor PTEN as Molecular Switch Node Regulating Cell Metabolism and Autophagy: Implications in Immune System and Tumor Microenvironment. Cells 2020;9:1725.
25. Kim M, Park J, Bouhaddou M, et al. A protein interaction landscape of breast cancer. Science 2021;374:eabf3066.
26. Yan XY, Zhang JJ, Zhong XR, et al. The LINC00365/SCGB2A1 (Mammaglobin B) Axis Down-Regulates NF-κB Signaling and Is Associated with the Progression of Gastric Cancer. Cancer Manag Res 2020;12:621-31.
27. Bellone S, Tassi R, Betti M, et al. Mammaglobin B (SCGB2A1) is a novel tumour antigen highly differentially expressed in all major histological types of ovarian cancer: implications for ovarian cancer immunotherapy. Br J Cancer 2013;109:462-71.
28. Munakata K, Uemura M, Takemasa I, et al. SCGB2A1 is a novel prognostic marker for colorectal cancer associated

with chemoresistance and radioresistance. Int J Oncol 2014;44:1521-8.
29. Tan S, Li D, Zhu X. Cancer immunotherapy: Pros, cons and beyond. Biomed Pharmacother 2020;124:109821.
30. Li BL, Wan XP. Prognostic significance of immune landscape in tumour microenvironment of endometrial cancer. J Cell Mol Med 2020;24:7767-77.
31. Pan K, Farrukh H, Chittepu VCSR, et al. CAR race to cancer immunotherapy: from CAR T, CAR NK to CAR macrophage therapy. J Exp Clin Cancer Res 2022;41:119.
32. Green AK, Feinberg J, Makker V. A Review of Immune Checkpoint Blockade Therapy in Endometrial Cancer. Am Soc Clin Oncol Educ Book 2020;40:1-7.
33. Paleari L, Pesce S, Rutigliani M, et al. New Insights into Endometrial Cancer. Cancers (Basel) 2021;13:1496.
34. Vermij L, Smit V, Nout R, et al. Incorporation of molecular characteristics into endometrial cancer management. Histopathology 2020;76:52-63.
35. Raffone A, Travaglino A, Raimondo D, et al. Lymphovascular space invasion in endometrial carcinoma: A prognostic factor independent from molecular signature. Gynecol Oncol 2022;165:192-7.
36. Di Donato V, Giannini A, Bogani G. Recent Advances in Endometrial Cancer Management. J Clin Med 2023;12:2241.
37. Cuccu I, D'Oria O, Sgamba L, et al. Role of Genomic and Molecular Biology in the Modulation of the Treatment of Endometrial Cancer: Narrative Review and Perspectives. Healthcare (Basel) 2023;11:571.
38. Yang X, Li X, Dong Y, et al. Effects of Metabolic Syndrome and Its Components on the Prognosis of Endometrial Cancer. Front Endocrinol (Lausanne) 2021;12:780769.
39. Socha MW, Malinowski B, Puk O, et al. C-reactive protein as a diagnostic and prognostic factor of endometrial cancer. Crit Rev Oncol Hematol 2021;164:103419.

Cite this article as: Zhang Y, Li L, Ke XP, Liu P. The identification of a PTEN-associated gene signature for the prediction of prognosis and planning of therapeutic strategy in endometrial cancer. Transl Cancer Res 2023;12(12):3409-3424. doi: 10.21037/tcr-23-1436

